Journal of Scientific & Industrial Research
Vol. 83, January 2024, pp. 15-24
DOI: 10.56042/jsir.v83i1.4148

XPM Induced Filter Free Multi-Wavelength Conversion Exploiting Hybrid Multiplexing Employing Sagnac Effect and Circulator in DWDM Networks

Parashuram[1,2] & Chakresh Kumar[1]*

[1]University School of Information, Communication and Technology, Guru Gobind Singh Indraprastha University, New Delhi 110 078, India

[2]Department of Electronics and Communications Engineering, Bharati Vidyapeeth's College of Engineering, Delhi 110 063

Received 19 July 2023; revised 08 November 2023; accepted 25 December 2023

In this paper, XPM based filter free wavelength conversion is proposed and demonstrated using Sagnac interferometric loop, circulator, asymmetric Mach-Zehnder modulators and multiplexers. Two input NRZ signals of different wavelengths (1551 nm and 1553 nm) each with a data rate of 100 Gb/s are simultaneously converted to a target wavelength of 1555 nm. In contrast to other interferometry, using a common route where two light beams propagate in opposite directions, the Sagnac interferometer uses the interference created by superimposing light waves to extract information. Sagnac effect is exploited to isolate the wavelengths as a frequency selector and to provide phase shift between co- and counter propagating signals. Proposed system is investigated with or without using the optical band passes filters and compared with the back-to-back (b2b) signal. Simulation results reveals that filter less conversion obtained higher extinction ratio (> 20 dB) for both 1551 nm to 1553 nm and 1553 to 1555 nm conversion using Sagnac effect. Power penalties are found to be less than 0.5 dB for the conversion of 1551 nm to 1555 nm and less than 0.4 dB for the conversion of 1553 nm to 1555 nm. To the best of our knowledge, this is a novel technique that provides filter-free wavelength conversion, multicasting, and a reduction in system complexity without requiring separate phase control. Even at low power, the lack of filters lowers bit error rate and insertion losses. Filter-free wavelength conversion lowers complexity, increases scalability, and is more stable.

Keywords: Group velocity dispersion, Highly nonlinear fiber, Interferometry, Nonlinearity, Semiconductor optical amplifier

Introduction

An all-optical Multi-Wavelength Conversion (MWC) is the backbone of nonlinear optics for fast processing. Wavelength converters are prominent devices for enabling dynamic routing and reuse of wavelength in futuristic advanced spectrally efficient DWDM networks. In recent times, several methods of wavelength conversion have been developed such as Periodically Poled Lithium Niobate (PPLN) waveguide, Pumping, Semiconductor Optical Amplifiers (SOAs), FWM, XGM, XPM, opto-electronic conversion. All these methods have many advantages and are effective, but there are some drawbacks as well. XGM based wavelength conversion implementing MQW-SOA is effective for converting 4- wavelengths at 40 Gb/s. It has limited operational speed as it depends on gain recovery time, carrier concentration rate in MQW-SOA, inverted coding operation and extinction ratio.[1] A PPLN wave guide-based wavelength conversion provides flexible tuning for different modulation formats using Cascaded Sum- and Difference Frequency Generation (cSFG/DFG) but it has some demerits such as pulse width adjustment and limiting bit rate.[2] Spectral filtering also plays key role in wavelength conversion using Self-Phase Modulation (SPM). Multicasting of converted signal inducing SPM on 100-m-long photonic-crystal-fiber medium has an advantage of not using polarization control and external light source but it is limited to 10-Gb/s Return-to-Zero (RZ) signal.[3] SOA-MZI interferometry is a good alternative for multi-wavelength conversion but phase control between different paths is a challenge at higher data rate which leads to limiting the number of channels.[4] FWM based wavelength conversion in a nonlinear medium provides sufficient tunable bandwidth range but FWM power adjustment is a key challenge as it is caused by third order nonlinearity and thus the Stimulated Brillouin Scattering (SBS) limits the line width of converted signal.[5] Raman assisted four-wave mixing can be exploited to realize all-optical multicasting switch at 10 Gb/s. It has some drawbacks such as uses of external light sources and limited pulse broadening on

*Author for Correspondence
E-mail: chakreshk@ipu.ac.in

dispersion shifted fiber.[6] Multicasting of DPSK signals using FWM over Bismuth Highly Nonlinear Fiber (Bi-HNLF) transmits information to multiple sources simultaneously but uses of three external sources (pumps) is a hurdle in matching the phase differences.[7] A format of wavelength conversion using Dispersion Shifted Highly Nonlinear Fiber (DS-HNLF) inducing XPM can attain large range of conversion bandwidth at high data rate.[8] More often high pump power is required to induce the XPM sufficiently owing to the lesser nonlinearity coefficient in DS-HNLF.

The All-Optical Wavelength Conversion (AOWC) has been conceptualized for 56 Gbps Polarization Division Multiplexing (PDM) 16-ary Quadrature Amplitude Modulation (QAM) signal exploiting FWM in dual polarization SOAs via configuration of the parallel State of Polarization (SOP) dual pumps.[9] This implementation has some limitations such as use of dual polarization to improve the bandwidth and spectral efficiency and a tradeoff among OSNR, injection current of SOA and pump power for long haul optical fiber communications which leads to the complexity of the system. The Photonic Crystal Fibers (PCFs) have various nonlinear optical processing such as dispersion compensators, lasers, amplifiers and wavelength conversion. The wavelength conversion over wide tunable range integrating the optofluidic infiltration of PCFs has been released correlating FWM and dispersion for pump wavelengths.[10] This process has difficulties in controlling the refractive index of the PCF air holes to tune with converted wavelength region. Graphene has some advantages over PCF in implementing FWM based polarization-controlled wavelength conversion but this approach has some disadvantages such as need of external dual pumping and SOP control unit.[11]

Sagnac interferometer-based fiber optic loop integrated on nonlinear fibers and circulators have found versatile functionality in optical regeneration, developing gyroscopes, wavelength (de) interleavers optical filters, pulse shaping, optical switching etc.[12–17] Sagnac interference can be a prominent alternative as compared to the other interferometry configuration for multi-wavelength conversion considering its utility. Sagnac interferometry provides a broader range of reflection band and high resilience in reflectance tuning. The utility of Sagnac effect has motivated researchers to look for other possible uses. Xu *et al*. have studied wavelength conversion employing Sagnac interferometric loop.[18] They have realized very less power penalty of 2.4 dB placing SOA at symmetric position. Extinction ratio has been improved due to correlative operation of cross-gain modulation and cross-polarization modulation effects. They have found that Sagnac interferometer can be enabled with the Terahertz Optical Asymmetric Demultiplexer (TOAD). This approach has some demerits such as less spectral efficiency and complexity in configuration. Zheng *et al*. have investigated frequency conversion using constructive interference in Sagnac loop.[19] They have modulated multifrequency modes correlating input-output in a large range of parameter values but lacking in terms of data rate and feasibility of data transmission to very limited number of channels. Fresnel rhomb has been used as a wideband and reasonable retarder in designing a Sagnac-type spontaneous parametric down conversion.[20] A good agreement of nondegenerate Entangled Photon Sources (EPS) has been concluded between both telecommunication wavelength and quantum-memory wavelength. This approach has some major drawbacks such as difficulties in controlling differences in phase shift and maintaining orthogonality due to multiple total internal reflections, stress-induced retardances. Menon *et al*. have demonstrated wavelength conversion using Sagnac interferometer based on asymmetric twin waveguide at 10 Gb/s and analyzed pulse shape of converted light beam.[21] They have used SOA offset to add the nonlinearity in interferometric loop and realized an undistorted performance over a long range of 30 nm window. It has many limitations such as less data rate, complexity in loop and appropriate positioning of SOA. Yan *et al*. have investigated frequency conversion using Sagnac interferometer.[22] They have realized that single photon conversion can lead to adequate amalgamation of quantum storage system with the quantum communication network. A compact all-optical wavelength converter has been investigated integrating an asymmetrically configured Sagnac loop and power penalty below 2.1 dB has been obtained.[23] 40 Gb/s NRZ data signal has been converted using Sagnac loop over the entire C-band and a comparative analysis for both up- and down-conversion has been made with respect to b2b configuration. Jiang *et al*. have demonstrated the all-optical wavelength conversion of 40 Gb/s NRZ signal using Sagnac loop interferometer.[24] They have correlated the SOA length and carrier characteristic

with the performance of Sagnac loop and observed that shorter length SOAs are more useful in the Sagnac interferometer. The main limitations of all such schemes are: wavelength dependence, less scalability, a smaller number of multicasting channels, complexity, more power requirement, and less operational speed. All these shortcomings motivate us to develop a wavelength conversion methodology which is simple and can incorporate a greater number of less spaced multicasting channels at higher data rates. We propose filter free wavelength conversion using Sagnac interferometry to reduce the complexity and to increase the scalability. Note that a filter contributes some insertion loss to external pumped light, which is undesirable. XPM based Sagnac interferometry using circulators is less prone to Amplified Spontaneous Emission (ASE). Moreover, externally tunable filters are not needed to extract the input data signal exactly in the proposed design. In this paper, we focus on the filter free multi-wavelength conversion of on-off driven Non-Return-to-Zero (NRZ) voltage data signals. This process involves the Cross-Gain Modulation (XGM) and the Sagnac effect on nonlinear fiber path.

Theoretical Analysis

This study presents a demonstration of the application of hybrid multiplexing. Hybrid multiplexing has been achieved by the use of circulator, Sagnac loop, fiber delays, and multiplexing. Signals are directed along predetermined pathways by a circulator, which controls the flow of signals. The circulator in the suggested network aids in managing signal routing between various components. In order to prevent signal interference, controlled fiber delays are used to control signal synchronization throughout the network. In order to exploit the available bandwidth and sustain high data rates, multiplexers are essential components of DWDM networks. They integrate several signals onto a single optical fiber. In order to improve signal quality, maximize performance, and add nonlinearity, XPM, and Sagnac interferometry inherence, hybrid multiplexing is employed. When used in DWDM networks, the Sagnac interferometer has a number of benefits, including built-in stability, ease of configuration, less crosstalk, improved signal quality, wavelength sensitivity, compatibility with optical fibers, and the possibility to use multiplexing techniques. The results and analysis section highlights some of the unique benefits of hybrid multiplexing, including resource optimization, performance optimization, flexibility, and adaptability.

Nonlinearity

The propagation of light beams in a dielectric medium results in nonlinearities for intense fields. Inside a medium, total induced polarization ($\vec{\mathcal{P}}$) in electric field ($\vec{\mathscr{E}}$) can be expressed as Eq. (1)

$$\vec{\mathcal{P}} = \epsilon_0\{\chi^1.\vec{\mathscr{E}} + \chi^2.\vec{\mathscr{E}}\vec{\mathscr{E}} + \chi^3.\vec{\mathscr{E}}\vec{\mathscr{E}}\vec{\mathscr{E}}\} \quad \ldots (1)$$

where, χ^k is the k[th] order susceptibility and permittivity of free space (vacuum) is denoted by ϵ_0. The first term in Eq. (1) represents linear polarization (dielectric constant) of total polarization and it contributes dominantly to $\vec{\mathcal{P}}$. Second and higher order terms contribute to nonlinear polarization. Second term represents the nonlinearity due to asymmetric nonlinear medium and vanishes for SiO_2 as it is a symmetric molecule. Effective refractive index (n_e) of nonlinear medium includes the combined effect of linearity and nonlinearity and it is related with mode intensity of light (I) as Eq. (2)

$$n_e = n_l + n_{nl}I \quad \ldots (2)$$

n_{nl} is the Kerr coefficient which is refractive index nonlinear coefficient. Dependance of the Kerr coefficient to the field intensity is known as Kerr effect. As intensity of light depends on the effective mode area A_e and input power P so effective refractive index of nonlinear medium is expresses as Eq. (3)

$$n_e = n_l + n_{nl}\frac{P}{A_e} \quad \ldots (3)$$

Linear refractive index of the fiber is written as Eq. (4)

$$n_l = \sqrt{1+\chi^1} \quad \ldots (4)$$

and, Nonlinear index coefficient is written as Eq. (5)

$$n_{nl} = \frac{3}{4}\frac{\chi^3}{c\epsilon_0 {n_l}^2} \quad \ldots (5)$$

Propagation of optical beam inside a single mode fiber (SMF) obeys the Nonlinear Schrodinger Equation (NLSE) as Eq. (6)

$$i\frac{\partial A}{\partial \xi} - \beta_2\frac{\partial^2 A}{\partial T^2} + i\frac{\alpha}{2}A = -\gamma|A|^2A \quad \ldots (6)$$

where, $A(\xi, T)$ is normalized amplitude of the pulse envelope, T is width (> 5ps) of the light pulses propagating inside the fibers. ξ is the direction of propagation, β_2 is the Group Velocity Dispersion (GVD) parameter and α is attenuation constant. Nonlinear coefficient γ is expressed as Eq. (7)

$$\gamma = \frac{\omega_o n_{nl}}{cA_e} \quad \ldots (7)$$

In Eq. (7), ω_o is central frequency, γ is nonlinearity propagation coefficient ($W^{-1}m^{-1}$), n_{nl} is nonlinear refractive index (Kerr coefficient), whereas A_e is the effective core area. On the basis of dispersion length (l_d), physical length of the fiber (l) and nonlinearity length (l_{nl}), four major situations arise. If $l_d \gg l$, and $l_{nl} \gg l$ then fiber acts just as a medium to transfer light without any nonlinear dispersive effects. If $l_d \ll l$, and $l_{nl} \gg l$ then dispersion pulse broadening incurs and GVD limited regime. For soliton, $l_d \ll l$, and $l_{nl} \ll l$. Moreover, for $l_d \gg l$, and $l_{nl} \ll l$ SPM incurs in a nonlinearity limited regime.

XPM

In XPM, the phase change of one beam in a nonlinear medium (a Kerr medium) is influenced by the optical intensity of another beam. Total electric field considering quasi-monochromatic approximation is written as Eq. (8)

$$\vec{\mathscr{E}}(r,t) = \frac{1}{2}\left[\mathscr{E}_1 e^{-i\omega_{o1}t} + \mathscr{E}_2 e^{-i\omega_{o2}t}\right]\hat{x} + c.c. \quad \ldots (8)$$

where, ω_{o1} and ω_{o2} are the central carrier frequencies of two light beam, polarization unit vector is denoted as $\hat{x}$, ω_{o1} and ω_{o2} are the carrier frequencies of the two optical beams and the corresponding optical field amplitudes $\mathscr{E}_1$ and $\mathscr{E}_2$ are slowly time varying functions compared with an optical period. In general, nonlinear effects in optical waveguides occurs using the short pulses assuming that spectral width of each light pulse obeys the condition $\Delta\omega_j << \omega_j$ $(j = 1,2)$ for widths ranging from ~10 ns to 10 fs. The maximum nonlinear phase contributed by SPM is expressed by the Eq. (9)

$$\phi_{nl} = \gamma P l_e \quad \ldots (9)$$

where, P is pulse input power and defined as $P = |A|^2$. For two channels, the nonlinear phase shift acquired by jth channel ($\phi_{nl,j}$) is stated as Eq. (10)

$$\phi_{nl,j}(\xi) = \gamma_j\left(P_j + 2P_{3-j}\right)\xi \quad \ldots (10)$$

where, $j = 1\ or\ 2$, and P_j is incident optical power for jth channel. Nonlinear coefficient for jth channel is defined as $\gamma_j = \frac{\omega_j n_{nl}}{cA_e}$ $(j = 1,2)$. Moreover, for the N-channel WDM system, Eq. (11) states the nonlinear phase shift that results from the superposition of SPM and XPM.

$$\phi_{nl,j} = \gamma_j l_e\left(P_j + 2\sum_{n\neq j}^{N} P_n\right) \quad \ldots (11)$$

where, l_e is effective length of the fiber and defined as $l_e = M\frac{1-e^{-\alpha L_A}}{\alpha}$, L_A is spacing for amplifier, α if fiber attenuation, and M is total number of sections integrated in whole fiber link. Considering only SPM and XPM effects for interaction of N WDM channels in an optical link, coupled differential equations for slowly varying amplitudes are expressed as Eq. (12)

$$\frac{\partial A_j}{\partial \xi} = -i\gamma_j\left(|A_j|^2 + 2\sum_{n\neq j}^{N}|A_n|^2\right)|A_j| \quad \ldots (12)$$

where, $j = 1\ to\ N$. A is slowly varying amplitude, ξ represents the distance travelled in propagation direction and γ_j is nonlinear coefficients for jth channel.

Sagnac Effect

The Sagnac interferometers were first reported for rotation sensing by George Sagnac in 1913. Nowadays, Sagnac interferometers have been implemented in sensing, lasing and optical communications. Some major applications of Sagnac effect in optical fiber communication systems are Interferometric Optical Gyroscopes (IOGs), reflective mirrors, wavelength (de) interleavers, filters and optical analogues of quantum physics. Sagnac effect states that the phase shift ($\triangle\phi$) between the counter-propagating light beams in an interferometer is related with a constant angular rotation rate ($\vec{\Omega}$) and expressed as Eq. (13)

$$\triangle\phi = \frac{8\pi E}{hc^2}\vec{A}.\vec{\Omega} \quad \ldots (13)$$

where, E is the accumulating energy of interfering particle and expressed as, $E = \frac{hc}{\lambda}$, λ is operating beam wavelength, speed of propagating beam in vacuum is represented as c, $\vec{A}$ is the area vector enclosed in the interferometer geometry, and h is the Planck's constant. Sagnac interferometers can also be used as wave length (de) interleavers for multiplexing and demultiplexing the signals in DWDM networks. Sagnac effect-based wavelength (de) interleavers can achieve high order filtering capability, roll-off with fewer units, high extinction ratio (ER) and precise flatness due to the co- and counter bidirectional light propagation maintaining stronger coherent mode interference.[25–27] Self-coupled Sagnac interferometer have been used to develop an integrated advance optical filter. Basics filters such as Chebyshev, Butterworth, elliptic and Bessel filters have been formed using Sagnac interference in order to achieve

both wavelength and bandwidth tuning, high extinction ratios and broad bandwidth.[28–30]

System Description and Operation

The proposed simulation setup for filter free wavelength conversion of two signals simultaneously each with a data rate of 100 Gb/s is shown in Fig. 1. The main essence of this design is the use of Sagnac effect, circulators and nonlinear fibers. A Continuous Wave (CW) laser source, namely cw_laser, generates probe signal at 1555 nm. Two input signals are Intensity Modulated (IM) separately at wavelengths 1551 nm (pump 1) and 1553 nm (pump 2) using cw_laser1 and cw_laser2 respectively. The intensity modulated signals are also known as pumps. Intensity modulation unit is comprised of the Pseudo Random Bit Sequence (PRBS) generator, the electrical signal generators (siggen) and the dual arm asymmetric Mach-Zehnder Modulator (MZM). PRBS1 and PRBS2 are used to generate a binary sequence of length $2^{31}-1$ for both input signal at 100 Gb/s. Logical signals are converted into electrical pulses using siggen1 and siggen2 for both input signals. Circulator is a 3 input and 3 output port device which is used to isolate light signals that propagate in opposite directions such that light signal does not exits from the same port at the output. Probe signal at desired wavelength of 1555 nm is fed to the input port 1 of the circulator. Optical signal of circulator at the output port 2 is coupled into the optical multiplexer 1 (OptMUX1) via time delay unit 1 (FiberDelay_1) and signal at the output port 3 of the circulator is coupled into the OptMUX2 via FiberDelay_2. Both the intensity modulated input data signals are coupled with probe signal using optical multiplexers. The optical delay in both fiber path has been used to maintain the Free Spectral Range (FSR) between two next to next transmission peaks. XPM is induced due to interaction of pump and probe light beams in a Kerr medium. After overlapping, optical intensity of one light alters the phase shift of others and XPM is governed by the Eqs (8–12). The outputs of both OptMUX1 and OptMUX2 are fed to the nonlinear fibers 1 (NLFiber1) and nonlinear fibers 2 (NLFiber2), respectively. Nonlinear fibers are used to convert the wavelengths of intensity modulated input data signals by using nonlinear factors such as Polarization Mode Dispersion (PMD), dispersion, XPM, ASE noise and bi-directional effects. The outputs of both device NLFiber1 and NLFiber 2 are fed to input port 1 and input port 2 of the Sagnac loop (named as Sagnac_Effect in Fig. 1), respectively. Sagnac effect generates a phase shift in a ring interferometer which depends on rotation. In a fiber

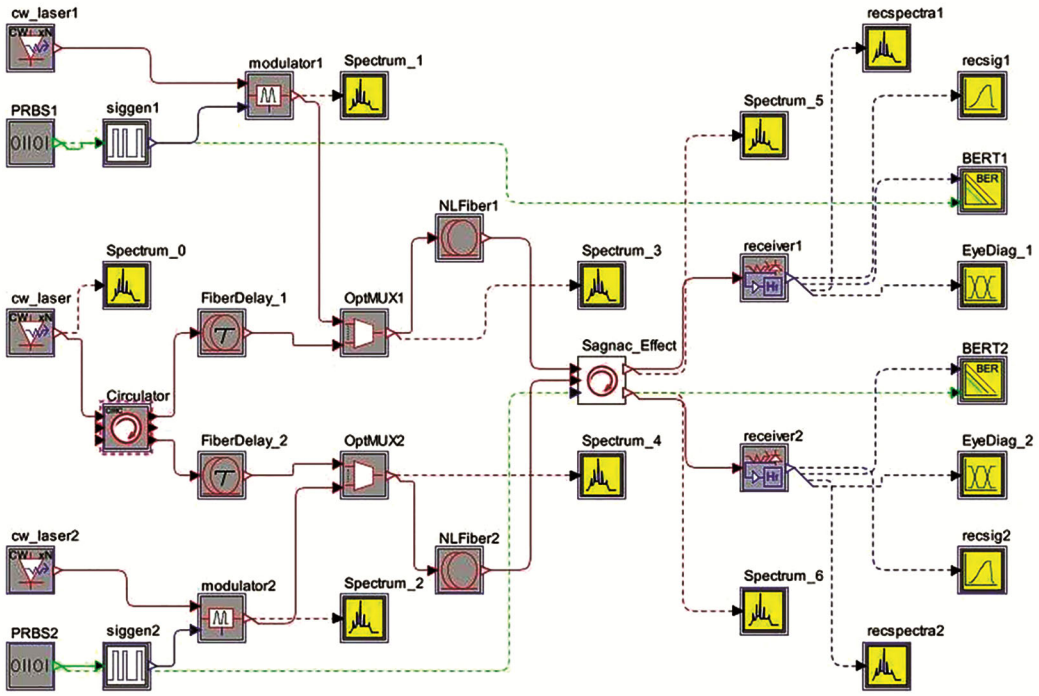

Fig. 1 — Simulation setups of proposed filter free wavelength conversion of two channels simultaneously employing Sagnac effect

optic loop, bidirectional Sagnac loop relates differential phase shift between clockwise and counter clockwise travelling light beams. Outputs of the Sagnac effect at outport 1 and outport 2 are fed to the optical receivers. Receiver1 detects the wavelength conversion of 1551 nm to 1555 nm and receiver2 detects the wavelength conversion of 1553 nm to 1555 nm wavelength conversion. Due to Sagnac effect, XPM induced wavelength converted signal, probe and pump signal are filtered out simultaneously in both nonlinear fiber paths without using external optical fibers. The performance of proposed system has been analyzed using optical spectrum analyzers, bit error rate tester (BERT1 and BERT2) and eye diagrams (EyeDiag_1 and EyeDiag_2).

Results and Discussion

The performance of proposed scheme of filter free wavelength conversion exploiting Sagnac effect is evaluated using optical spectrum analyser, optical receiver, bit-error-rate tester (BERT) and eye-diagrams. Simulations are performed in OptSim software. Simulation parameters of nonlinear fiber are followed as- length: 10 Km, loss inside the f iber: 0.2 dB/km, dispersion: 1.4×10^{-6} m, pmd coefficient: 3.16×10^{-15} s/m$^{0.5}$, and coil diameter of Sagnac loop: 3.2 cm. Moreover, parameters of optical receiver integrated with Avalanche Photo-Diode (APD) detector are taken as: pre-bits: 2, post-bits: 3, photodetector quantum efficiency: 0.8, and bandwidth (BW): 10 GHz.

The intensity-modulated input signal (pump signal) at 1551 nm via cw_laser1 and the probe signal at 1555 nm via cw_laser and circulator are coupled, and the resulting optical spectrum is displayed in Fig. 2(a). This spectrum displays the power received at the OptMUX1 output over a range of wavelengths for 0 dBm probe power and −10 dBm pump power. The optical spectrum for the 1551 nm to 1555 nm wavelength conversion via nonlinear route NLFiber1 at −10 dBm probe power and −30 dBm pump power is displayed at output port 1 of the Sagnac effect block in Fig. 2(b). This figure displays that input signal at 1551 nm has been shifted to targeted wavelength of 1555 nm. Converted signal is centered at 1555 nm for a broader wavelength span and power strength increases by 10 dBm due to cross-gain modulation (XGM) in nonlinear path. Sagnac effect has been occurred to isolate the frequency of both transmitted and targeted signal.

After connecting an intensity-modulated input signal (pump signal) at 1553 nm via cw_laser2 and a probe signal at 1555 nm via cw_laser and circulator, the optical spectrum produced from OptMUX2 is shown in Fig. 3(a). This spectrum displays, with a launch power of 0 dBm for the probe and −10 dBm for the pump, the optical power received at the OptMUX2's output across a range of wavelengths.

The optical spectrum for the 1553 nm to 1555 nm wavelength conversion via nonlinear route NLFiber2 at −10 dBm probe power and −30 dBm pump power is displayed at output port 2 of the Sagnac effect block in Fig. 3(b). This figure displays that input signal at 1553 nm has been shifted to targeted wavelength of 1555 nm. Converted signal is centered at 1555 nm for a much broader wavelength span and power strength increases by 12 dBm due to cross-gain modulation (XGM) in nonlinear path. Sagnac effect has been occurred to isolate the centered frequency of both transmitted and targeted signal at 1553 nm and 1555 nm respectively. Both Fig. 2(b) and Fig. 3(a) confirm that Sagnac interferometer plays an important role for frequency selection and filtering due to phase shift of propagating signals in a fiber optic loop for both the simultaneous conversions without using any

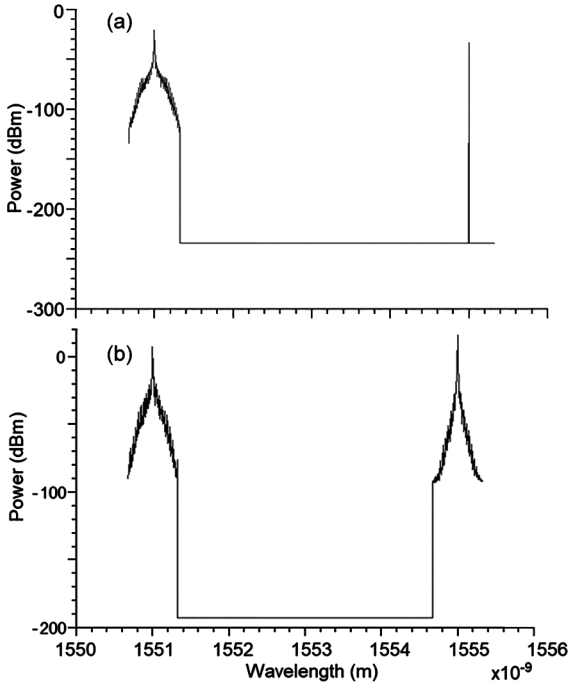

Fig. 2 — Optical spectra for 1551 to 1555 nm wavelength conversion: (a) at the output port of OptMUX1 (b2b signal spectra); and (b) at the output port 1 of Sagnac loop (wavelength converted signal spectra)

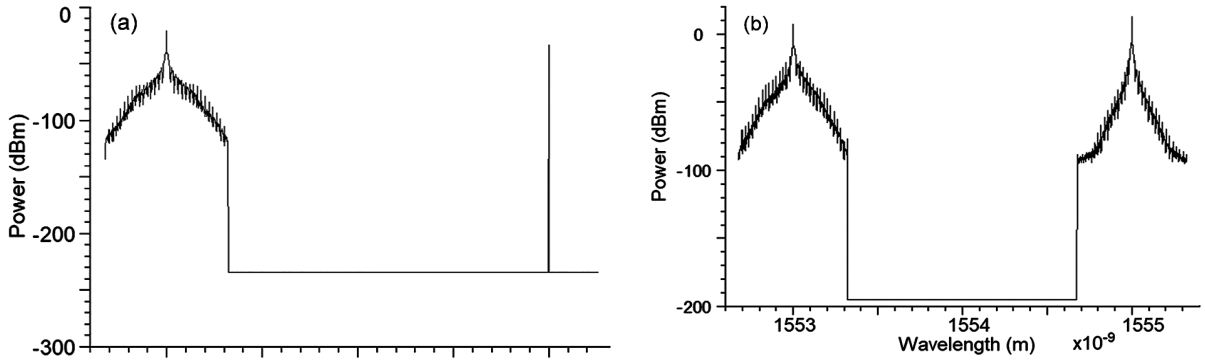

Fig. 3 — Optical spectra for 1553 to 1555 nm wavelength conversion (a) at the output port of OptMUX2 (b2b signal spectra); and (b) at the output port 2 of Sagnac loop (wavelength converted signal spectra)

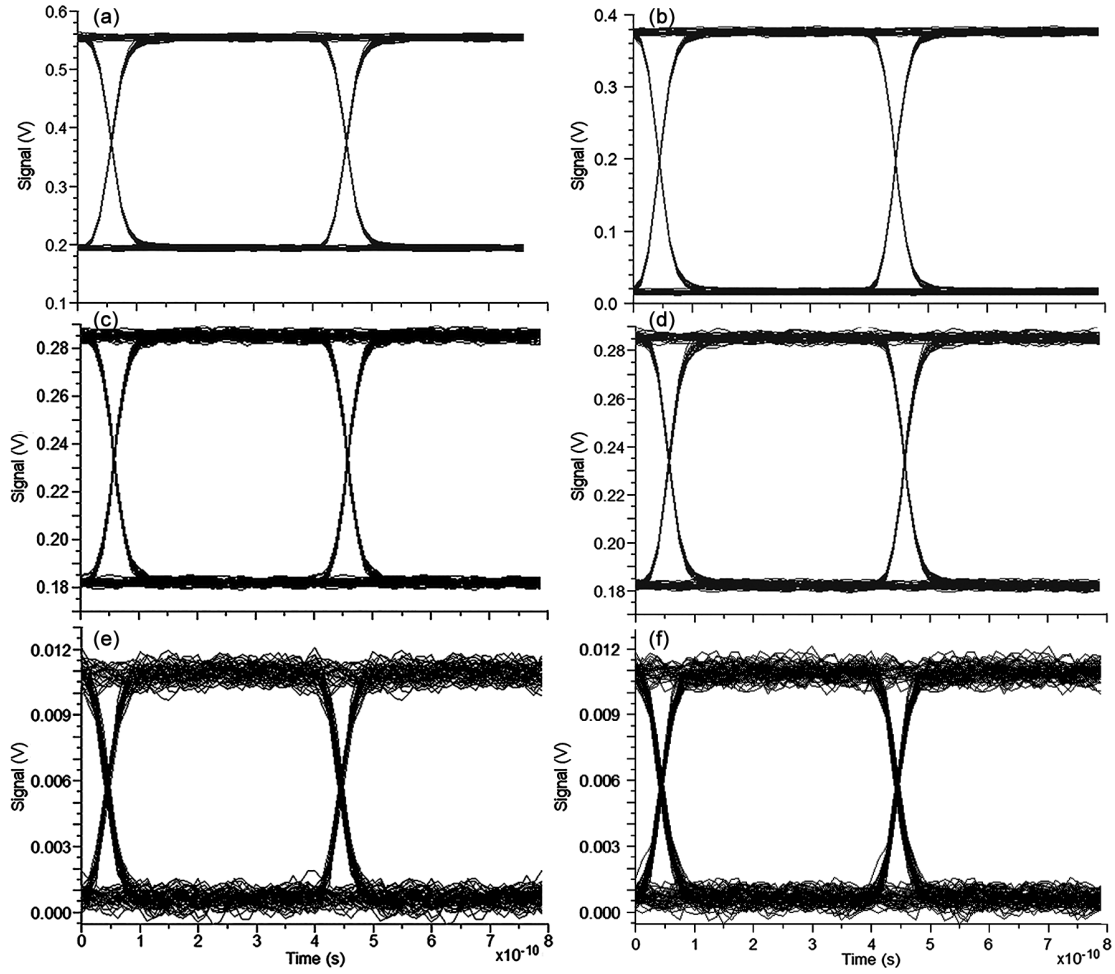

Fig. 4 — Eye diagram (a) at 1551 nm before conversion (b2b signal) at 0 dBm probe power and −10 dBm pump power; (b) for 1551 to 1555 nm wavelength conversion with filter at −10 dBm probe power and −30 dBm pump power; (c) for 1551 to 1555 nm wavelength conversion without filter at −10 dBm probe power and −30 dBm pump power; (d) at 1553 nm before conversion (b2b signal) at 0 dBm probe power and −10 dBm pump power; (e) for 1553 to 1555 nm wavelength conversion with filter at −10 dBm probe power and −30 dBm pump power; and (f) for 1553 to 1555 nm wavelength conversion without filter at −10 dBm probe power and −30 dBm pump power

external optical filter. Signal strength due to XPM in both the path is governed by the Eq. (12) and Sagnac effect is governed by the Eq. (13).

The b2b eye diagram for an NRZ input data signal at 1551 nm at 0 dBm probe signal strength and −10 dBm pump signal power is displayed in Fig. 4(a).

The eye diagrams for wavelength conversion of 1551 nm to 1555 nm with and without the use of a filter, respectively, at −10 dBm probe signal power and −30 dBm pump signal power, are shown in Fig. 4(b) and 4(c). From both the Fig. 4(b) and Fig. 4(c), it has been observed that obtained optical field strength of converted signal is very high at very low launch power of input signal. A wide-open eye-diagram is realized without using filter as shown in Fig. 4(c). Comparing the eye-diagrams of Fig. 4(a) and Fig. 4(c), it can be concluded that there is no pulse-broadening after wavelength conversion even without using filters which reflects a very fast conversion. Furthermore, Fig. 4(d), Fig. 4(e) and Fig. 4(f) show the eye diagrams of back-to-back signal, after conversion with filter and after conversion without filter, respectively, for 1553 nm to 1555 nm. The eye diagram is displayed in Fig. 4(d) at 0 dBm probe power and −10 dBm pump power prior to conversion. The eye diagrams at −10 dBm probe power and −30 dBm pump power, following wavelength conversion, are displayed in Fig. 4(e) and 4(f). Comparing the eye-diagrams of Fig. 4(e) and Fig. 4(f), it is observed the performance of conversion is comparable with and without filter and there is no pulse-broadening even without using optical filter which reflects a very fast conversion for 1553 nm to 1555 nm conversion also. Eye diagrams analysis confirms that Sagnac interferometer can reduce the complexity of design and improve the performance without using the filters.

The bit-error-rate (BER) curves for the wavelength conversion from 1551 nm to 1555 nm are displayed in Fig. 5(a) as a function of the received power. Bit-error-rates of b2b and converted signal with or without filter measured using BER tester BERT1 via optical receiver1 are shown at launch power of −10 dBm probe and −30 dBm pump. The BER decreases as received power increases. Launched power of both probe and pump signal is correlated to BER. Received power obtained for b2b signal, converted signal with filter and converted signal without filter at $\mathrm{BER} = 10^{-9}$ are −36.8 dBm, −35.8 dBm and −34.3 dBm, respectively. It is observed that power penalties are less than 1.5 dB for high data rate 100 Gb/s NRZ signal which can be reduced below 0.5 dB for data rate less than 60 Gb/s. The BER curves as a function of the received power for 1553 nm to 1555 nm wavelength conversion are shown in Fig. 5(b). Bit-error-rates of b2b signal before conversion and converted signal with or without filter measured using BER tester BERT2 via optical receiver 2 are displayed at launch power of −10 dBm probe and −30 dBm pump. Received power obtained for b2b signal, converted signal with filter and converted signal without filter at $\mathrm{BER} = 10^{-9}$ are −36.4 dBm, −35.2 dBm and −34.2 dBm, respectively. It is observed that power penalties are below 1.5 dB at higher data rate of 100 Gb/s which can be further improved by optimizing the launch power and reducing the data rate. For data rate less than 60 Gb/s, power penalties can be lowered to below 0.4 dB

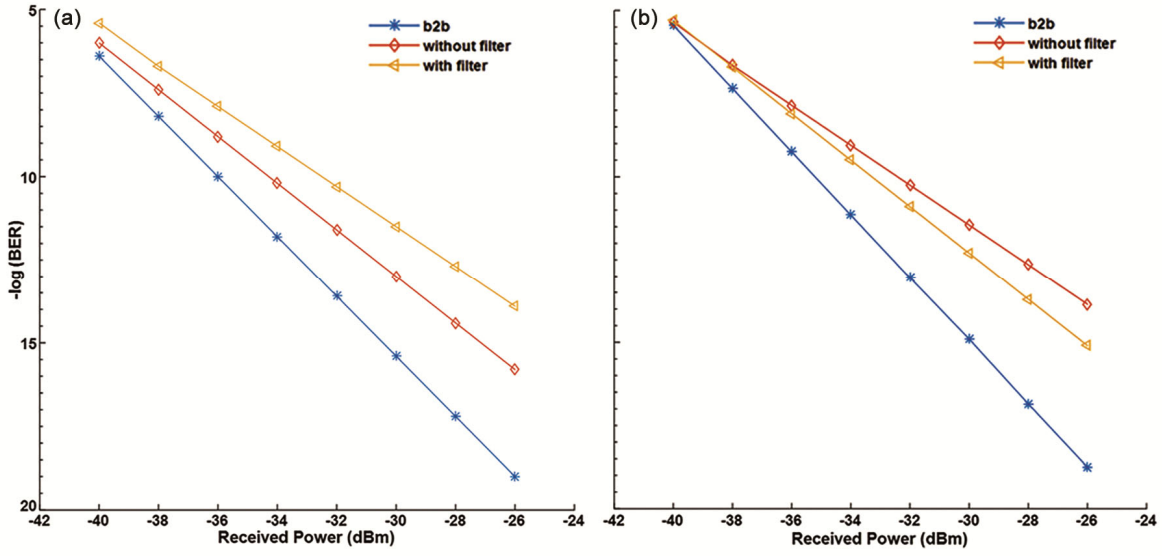

Fig. 5 — BER curves for wavelength conversion without filter at −10 dBm probe power, and −30 dBm pump power (a) 1551 to 1555 nm; and (b) 1553 to 1555 nm

Table 1 — Comparative analysis of proposed work with recent research pertained to wavelength conversion

Parameters	Parashuram *et al*.[1]	Pakarzadeh *et al*.[10]	Jiang *et al*.[24]	Jansen *et al*.[23]	Xu *et al*.[18]	Yang *et al*.[11]	Zhao *et al*.[9]	Present Work
Input signal type	CW Laser	Pumped	Pumped NRZ signal	NRZ data signal	DFB	Tunable Laser	PDM–16QAM	NRZ intensity modulated
Probe signal type	DRZ modulated	PCF (Photonic Crystal Fibers)	CW	CW	DFB	DFB-LD	CW	CW
Input signal wavelength	1525 nm, 1535 nm, 1545 nm, 1555 nm	1513 nm	1558 nm	1545 nm	1548.5 nm	1550.89 nm, 1551.32 nm	193.38 THz, 193.43 THz	1551 nm, 1553 nm
Converted wavelength	1540 nm	0.6μ–2μ	1550 nm	1540 nm, 1560 nm	1544.4 nm	—	192.13 THz, 192.34 THz	1555 nm
Technology	XGM in MQW-SOA	Optofluidic infiltration in PCF, SMI based on FWM	Sagnac loop, XPM, XGM in SOA	Asymmetric Sagnac loop	Sagnac Interferrometric loop with TOAD, XPM, XGM	FWM on Graphen, Dual Pumps	FWM in SOA, Parallel dual pumps	Sagnac Effect (without filter), XPM in Nonlinear Fiber, Circulator
Data rate	40 Gb/s	—	40 Gb/s	42.7 Gb/s	—	—	56 G-baud	100 Gb/s
Performance measurement	CE = 30 dB, ER >15 dB	Wavelength shift of 2326.6 nm at 1.32 refractive index	Gain > 25 dB	Power penalty < 2.1 dB, BER < 10^{-12}	Power Penalty < 2.4 dB	CE = 8 dB	OSNR Penalty = 2dB	ER > 20 dB, Power penalty < 1.5 dB at 100 Gb/s, < 0.4 dB at 60 Gb/s
Polarization effect	Independent	—	—	Independent	—	Independent	Independent	—
Multiplexing	Optical multiplexer (4:1)	—	Coupler	Coupler	Coupler	Coupler (50:50)	PBC, PBS	Optical multiplexer, Circulator

at 1553 nm. For both conversion extinction ratio (ER) is > 20 dB without using filter for high data rate 100 Gb/s NRZ signal. BER is improved for 1553 nm pump input signal comparing to 1551 nm pump signal as there is less frequency gap between input data signal (1553 nm) and targeted signal (1555 nm).

Furthermore, Table 1 shows the comparative analysis of proposed work with recent investigations attributed to wavelength conversion.

Conclusions

Filter free wavelength conversion of 100 Gb/s NRZ signal has been demonstrated inducing XPM by Sagnac loop on nonlinear fiber path. Sagnac effect is used to select the targeted wavelength correlating the phase shift between counter propagating optical beam. It provides better phase control, high scalability, and more tuning flexibility. The results show that it is possible to convert two wavelengths concurrently and efficiently without the need for filters. For both conversions obtained Extinction Ratio (ER) is higher than 20 dB. Additionally, Power penalty is less than 0.5 dB power penalties for 1551 nm to 1555 nm conversion and less than 0.4 dB for 1553 nm to 1555 nm at 60 Gb/s. Furthermore, the number of filter free conversions over existing system can be extended by optimizing interferometry and can be investigated for RZ signal also at high speed. Sophisticated techniques may yield improved conversion efficiency since insertion losses can be caused by circulators and the Sagnac effect. Since the wavelength range at which conversion is efficient may be limited by the properties of the nonlinear media utilized in the Sagnac loop, a tradeoff between wavelength and speed is necessary.

References

1 Parashuram & Kumar C, An optimal approach of bidirectional multiwave length conversion based on XGM in MQW-SOA, *IEEE Xplore* (IEEE) 2023, 22927938, https://doi.org/10.1109/PIECON56912.2023.10085858.

2 Wang J, Sun J, Luo C & Sun Q, Flexible all-optical wavelength conversions of 1.57-ps pulses exploiting cascaded sum- and difference frequency generation (cSFG/DFG) in a PPLN waveguide, *Appl Phys B: Lasers Opt*, **83** (2006) 543–548, https://doi.org/10.1007/s00340-006-2240-z.

3 Kwok C H, Lee S H, Chow K K, Shu C, Lin C & Bjarklev, Polarization-insensitive all optical wavelength multicasting by self phase-modulation in a photonic-crystal fiber, *IEEE Xplore, Proc of CLEO 2006* (Long Beach, CA*)* 2006, http://dx.doi.org/10.1109/CLEO.2006.4628166.

4 Yan N, Jung H D, Monroy I T, Waardt H D & Koonen T, All-optical multi-wavelength conversion with negative power penalty by a commercial SOA-MZI for WDM wavelength multicast, *Proc of OFC* (IEEE) 2007.

5 Zhang A & Demokan M S, Broadband wavelength converter based on four-wave mixing in a highly nonlinear photonic crystal fiber, *Opt Lett*, **30(18)** (2005) 2375–2377, https://doi.org/10.1364/OL.30.002375.

6 Lau K, Wang S H, Xu L, Lu C, Tam H Y & Wai P K A, All-optical multicast switch employing Raman-assisted FWM in dispersion-shifted fiber, *IEEE Photon Technol Lett*, **20(20)** (2008) 1730–1732, https://doi.org/10.1109/LPT.2008.2004565.

7 Lu G W, Abedin K S & T Miyazaki, DPSK multicast using multiple-pump FWM in Bismuths highly nonlinear fiber with

high multicast efficiency, *Opt Express*, **16(26)** (2008) 21964–21970, https://doi.org/10.1364/OE.16.021964.

8 Krcmarik D, Karasek M, Radil J & Vojtech J, Multi-wavelength conversion at 10 Gb/s using cross-phase modulation in highly nonlinear fiber, *Opt Commun*, **278(2)** (2007) 402–412, https://doi.org/10.1016/j.optcom.2007.06.004.

9 Zhao Y, Yan Z, Fu P, Cai Y & Yuan Y, All-optical wavelength conversion based on dual-polarization SOAs for a 112Gbps PDM-16QAM signal using parallel dual-pump, *OSA Continuum*, **4(4)** (2021) 1125–1134, https://doi.org/10.1364/OSAC.415288.

10 Pakarzadeh H, Derakhshan R & Hosseinabadi S, Tunable wavelength conversion based on optofluidic infiltrated photonic crystal fibers, *J Nonlinear Opt Phys Mater*, **28(01)** (2019) 1950002, https://doi.org/10.1142/S0218863519500024.

11 Yang Y, Duan M, Lin J, Wang Z, Wang K, Ji J & Song Y, Graphene-enhanced polarization-insensitive all-optical wavelength conversion based on four-wave mixing, *Opt Express*, **30(6)** (2022) 10168–10177, https://doi.org/10.1364/OE.452853.

12 Zhirnov A A, Choban T V, Stepanov K V, Koshelev K I, Chernutsky A O, Pnev A B & Karasik V E, Distributed Acoustic Sensor Using a Double Sagnac Interferometer Based on Wavelength Division Multiplexing, Pervasive Fiber Optic Sensor Technology: Improvements and Applications, *Sensors*, **22(7)** (2022) 2772, https://doi.org/10.3390/s22072772.

13 Arianfard H, Wu J, Juodkazis S & Moss D J, High performance optical filters based on advanced coupled Sagnac loop waveguide reflector structures, *Proc SPIE 11691, Silicon Photonics XVI*, **11691** (2021) 1169107, https://doi.org/10.1117/12.2584020.

14 Papadopoulos G & Zoiros K E, On the design of semiconductor optical amplifier-assisted Sagnac interferometer with full data dual output switching capability, *Opt Laser Technol*, **43(3)** (2011) 697–710, https://doi.org/10.1016/j.optlastec.2010.09.012.

15 Arianfard H, Wu J, Juodkazis S & Moss D J, Three Waveguide Coupled Sagnac Loop Reflectors for Advanced Spectral Engineering, *J Light Technol*, **39(11)** (2021) 3478–3487.

16 Ma M, Chen H, Zhang W, Li S & Jing X, Temperature sensor based on a Sagnac interferometer using a liquid crystal-filled microstructured optical fiber, *Mater Res Express*, **6(8)** (2019) 085205.

17 Arianfard H, Juodkazis S, Moss D & Wu J, Sagnac interference in integrated photonics featured, *Appl Phys Rev*, **10(1)** (2023) 011309, https://doi.org/10.1063/5.0123236.

18 Xu L, Glesk I, Baby V & Prucnal P R, All-optical wavelength conversion using SOA at nearly symmetric position in a fiber-based sagnac interferometric loop, *IEEE Photon Technol Lett*, **16(2)** (2004) 539–541, https://doi.org/10.1109/LPT.2003.821051.

19 Zheng A, Zhang G, Gui L & Liu J, Single-photon frequency conversion and multi-mode entanglement via constructive interference on Sagnac loop, *Laser Phys*, **25(6)** (2015) 065201, http://dx.doi.org/10.1088/1054-660X/25/6/065201.

20 Aizawa N, Niizeki K, Sasaki R & Horikiri T, Sagnac interferometer-type nondegenerate polarization entangled two-photon source with a Fresnel rhomb, *Appl Opt*, **62(9)** (2023) 2273–2277, https://doi.org/10.1364/AO.484456.

21 Menon V M, Tong W, Li C, Xia F, Glesk I, Prucnal P R & Forrest S R, All-optical wavelength conversion using a regrowth-free monolithically integrated Sagnac interferometer, *IEEE Photon Technol Lett*, **15(2)** (2003) 254–256, http://dx.doi.org/10.1109/LPT.2002.806888.

22 Yan W, Huang J & Fan H, Tunable single-photon frequency conversion in a Sagnac interferometer, *Sci Rep*, **3(1)** (2013) 3555, http://dx.doi.org/10.1038/srep03555.

23 Jansen S L, Chayet H, Granot E, Ezra S B, Borne D D V, Krummrich P M, Chen D, Khoe G D & Waardt H D, Wavelength conversion of a 40-gb/s NRZ signal across the entire C-band by an asymmetric Sagnac loop, *IEEE Photon Technol Lett*, **17(10)** (2005) 2137–2139, https://doi.org/10.1109/LPT.2005.854427.

24 Jiang X, Wang J, Gao C, Xu J & Wan H, All-optical NRZ wavelength conversion using a Sagnac loop with optimized SOA characteristics, *J Semicond*, **36(1)** (2015) 014013, http://dx.doi.org/10.1088/1674-4926/36/1/014013.

25 Li X P, Chen K X & Wang L F, Compact and electro-optic tunable interleaver in lithium niobate thin film, *Opt Lett*, **43(15)** (2018) 3610–3613, https://doi.org/10.1364/ol.43.003610.

26 Mizuno T, Oguma M, Kitoh T, Inoue Y & Takahashi H, Lattice-form CWDM interleave filter using silica-based planar lightwave circuit, *IEEE Photon Technol Lett*, **18(15)** (2006) 1570–1572, 2006, https://doi.org/10.1109/LPT.2006.878149.

27 Jiang X, Yang Y, Zhang H, Peng J, Zhang Y, Qiu C & Su Y, Design and experimental demonstration of a compact silicon photonic interleaver based on an interfering loop with wide spectral range, *J Light Technol*, **35(17)** (2017) 3765–3771, https://doi.org/10.1109/JLT.2017.2720188.

28 Zumbahlen H, Analog filters, *Linear Circuit Design Handbook* (Newnes, Burlington) 2008, 581–679, Hardback ISBN: 9780750687034, eBook ISBN: 9780080559155.

29 Jiang X, Wu J, Yang Y, Pan T, Mao J, Liu B, Liu R, Zhang Y, Qiu C, Tremblay C & Su Y, Wavelength and bandwidth-tunable silicon comb filter based on Sagnac loop mirrors with Mach–Zehnder interferometer couplers, *Opt Express*, **24(3)** (2016) 2183–2188, https://doi.org/10.1364/OE.24.002183.

30 Ge R, Luo Y, Gao S, Han Y, Chen L & Cai X, Reconfigurable silicon bandpass filters based on cascaded Sagnac loop mirrors, *Opt Lett*, **46(3)** (2021) 580–583, https://doi.org/10.1364/OL.410477.